Short Time Scale Dynamics and a Second Correlation between Liquid and Gas Phase Chemical Rates: Diffusion Processes in Noble Gas Fluids

Pelin Cox and Steven A. Adelman*

Department of Chemistry, Purdue University, West Lafayette, Indiana 47907-2084, United States

Received: August 6, 2010; Revised Manuscript Received: October 13, 2010

A theoretical formula for single-atom diffusion rates that predicts an isothermal correlation relation between the liquid (l) and gas (g) phase diffusion coefficients, $D(T, \rho_l)$ and $D(T, \rho_g)$ is developed. This formula is based on a molecular level expression for the atom's diffusion coefficient, $D(T, \rho)$, and on numerical results for 1715 thermodynamic states of 25 rare gas fluids. These numerical results show that at fixed temperature, T, the decay time, τ_{DIF}, which governs the shortest time decay of an appropriate force autocorrelation function, $\langle F(t)\, F\rangle_0$, is density ($\rho$)-independent. This independence holds since τ_{DIF} arises from the ρ-independent shortest time inertial motions of the solvent. The ρ independence implies the following l−g diffusion coefficient correlation equation: $D^{-1}(T, \rho_l) = (\rho_l/\rho_g)\, D^{-1}(T, \rho_g)\, [\rho_l^{-1}\langle F_{0,l}^2\rangle/\rho_g^{-1}\langle F_{0,g}^2\rangle]$. This relation is identical in form to the familiar (isolated binary-collision-like) empirical correlation formula for vibrational energy relaxation rate constants. This is because both correlation relations arise from inertial dynamics. Inertial dynamics always determines short-time fluid motions, so it is likely that similar correlation relations occur for all liquid phase chemical processes. These correlation relations will be most valuable for phenomena dominated by short time scale dynamics.

I. Introduction

Gas and dense fluid chemical rates can be related theoretically if the underlying force autocorrelation functions (faf) are isothermally density (ρ)-independent at the shortest times. For example, we have shown earlier[1] that the empirical correlation relation[2] between liquid (l) and gas (g) phase vibrational energy relaxation (VER) rate constants

$$k(T, \rho_l) = \left(\frac{\rho_l}{\rho_g}\right) k(T, \rho_g)\, G \tag{1.1}$$

(where G is of order unity) may be derived from the short-time ρ independence of the relaxing mode's faf $\langle F(t)\, F\rangle_0$.[3]

We propose here that liquid−gas (l−g) correlation relations such as eq 1.1 are not limited to VER. Rather, we give evidence that suggests that similar relations exist for many chemical processes (for example, activated barrier crossing). This is so since short-time-scale ρ independence is likely to hold widely in solution chemistry (see section V).

Specifically, we prove that the l−g rate correlation extends to a second process, the diffusion[4] of rare gas solutes present at infinite dilution in pure rare gas solvents. We do this by showing numerically that for these diffusion processes, short-time isothermal ρ independence holds for 1715 thermodynamic states of the 25 possible systems.

Our plan here is as follows: In section II we first write down our basic equations. Especially, we define the solvent decay times, τ, which determine the short-time behavior of the faf's for VER (τ_{VER}) and diffusion (τ_{DIF}). In section III, we first review the isothermal ρ independence principle for VER. Then we show isothermal ρ independence of τ_{DIF} for our 25 rare gas diffusion systems at temperature $T = 300$ K. In section IV we extend this 300 K study to many other Ts for a few selected systems. Especially, we study τ_{DIF} for He−He and Xe−Xe, the most divergent diffusion systems, over the supercritical ranges of their phase diagrams. Finally, in section V we derive the l−g correlation relation for diffusion coefficients and identify the liquid phase inertial motions[5] as the source of the ρ independence of τ.

II. Basic Equations and Their Numerical Evaluation

Here, we summarize the equations and the numerical methodology used later.

a. faf's and the Decay Time, τ. All normalized classical faf's $C(t) \equiv \langle F^2\rangle_0^{-1}\, \langle F(t)\, F\rangle_0$ have the rigorous time series representation

$$C(t) = 1 - \frac{1}{2!}\frac{\langle \dot{F}\dot{F}\rangle_0}{\langle F^2\rangle_0}t^2 + \frac{1}{4!}\frac{\langle \ddot{F}\ddot{F}\rangle_0}{\langle F^2\rangle_0}t^4 + \ldots \tag{2.1}$$

Defining the decay time τ by

$$\tau = \left[\frac{\langle F^2\rangle_0}{\langle \dot{F}^2\rangle_0}\right]^{1/2} \tag{2.2}$$

and truncating eq 2.1 to order t^2 yields

$$C(t) \doteq 1 - \frac{1}{2}\frac{t^2}{\tau^2} \tag{2.3}$$

Equation 2.3 diverges as $t \rightarrow \infty$ and thus is not a valid model for $C(t)$. Most valid models, however, do reduce to eq 2.3 to

* To whom correspondence should be sent. Phone: (765) 494-5277. Fax: (765) 494-0239. E-mail: saa@purdue.edu.

10.1021/jp1074175
Published on Web 11/08/2010

order t^2. For example, this reduction holds for the Gaussian model faf,

$$C_G(t) \equiv \exp\left(-\frac{1}{2}\frac{t^2}{\tau^2}\right) \tag{2.4}$$

Moreover, from eq 2.4, τ may be interpreted a faf's Gaussian decay time.

b. Quadrature Formulas for τ_{VER} and τ_{DIF}. For both VER and diffusion in monatomic solvents, the parameters $\langle F^2\rangle_0$ and $\langle \dot{F}^2\rangle_0$ and, hence, by eq 2.2, the corresponding τ's may be reduced to integrals over solute−solvent radial distribution functions $g(r)$ and pair potentials $u(r)$.[6,7]

We next review the integral formulas for these parameters. Our main intent is to show that isothermal ρ independence emerges from both the VER and diffusion integral formulas, despite the fact that the two sets of formulas are very different. This common emergence indicates that ρ independence of τ reflects fundamental principles. We start with the VER formulas.

(i) Formulas for the VER Gaussian Parameters. Even for the simplest case of diatomic solutes in monatomic solvents, the expressions for the VER parameters are complex.[6] This is especially so for$\langle \dot{F}^2\rangle_0$, so here, we give only the formula for$\langle F^2\rangle_0$, since this is sufficient to give a good impression of the nature of the full set of VER integral formulas.

For a diatomic solute with atomic coordinates $\mathbf{r_1}$ and $\mathbf{r_2}$ and masses m_1 and m_2, the integral formula for $\langle F^2\rangle_0$ is the following double sum over the solute atom indices i and j.

$$\langle F^2\rangle_0 = 3(m_1 + m_2)^{-1}\sum_{i=1}^{2}\sum_{j=1}^{2} T^{ij} I_{ij} \tag{2.5}$$

where

$$T^{ij} \equiv (-)^{i+j}\frac{1}{3}\left(\frac{m_1 m_2}{m_i m_j}\right) \tag{2.6}$$

and where I_{ij} is an integral over the radial distribution functions $g_{i(j)}(r)$ and potentials $u_{i(j)}(r)$ linking solute atom $i(j)$ with a solvent atom; namely,

$$I_{ij} = \rho^2 \int_0^{2\pi} \mathrm{d}\varphi \int_0^{\pi} \sin\theta\, \mathrm{d}\theta \int_0^{\infty} q^2\, g_i(y_i)\, g_j(y_j)\, A_{ij}(\mathbf{y}_i, \mathbf{y}_j)\, \mathrm{d}q \tag{2.7}$$

In eq 2.7 $\mathbf{q} = (q, \theta, \varphi)$ is the solvent atom's vector displacement from the solute's center of mass, while $\mathbf{y}_{i(j)} = \mathbf{q} - \mathbf{r}_{i(j)}$ is the vector displacement of the solvent atom from solute atom $i(j)$. In addition, assuming the solute molecule is aligned along the Z-axis (unit vector $\mathbf{e}_z$), $A_{ij}(\mathbf{y}_i, \mathbf{y}_j)$ in eq 2.7 is

$$A_{ij}(\mathbf{y}_i, \mathbf{y}_j) = [\mathbf{e}_z\cdot\mathbf{i}][\mathbf{e}_z\cdot\mathbf{j}]\, u_i'(y_i)\, u_j'(y_j) \tag{2.8}$$

where $y_{i(j)} = |\mathbf{y}_{i(j)}|$ and $\boldsymbol{i(j)} = [y_{i(j)}]^{-1}\,\mathbf{y}_{i(j)}$. The dot products $\mathbf{e}_z\cdot\mathbf{i(j)}$ are the following functions of $y_{i(j)}$, of $r_{i(j)} = |\mathbf{r}_{i(j)}|$, and of (q, θ, φ)

$$[\mathbf{e}_z\cdot\mathbf{i(j)}] = {y_{i(j)}}^{-1}[q\cos\theta - r_{i(j)}] \tag{2.9}$$

TABLE 1: Lennard-Jones (LJ) Parameters for the Systems Studied Here

atomic pair	σ (Å)	ε (K)
H(D)−Ar	1.39	25.40
Xe−Xe	4.10	222.00
Kr−Xe	3.97	190.81
Ar−Xe	3.76	163.22
Ne−Xe	3.43	88.90
He−Xe	3.33	47.63
Kr−Kr	3.83	164.00
Ar−Kr	3.62	140.29
Ne−Kr	3.29	76.41
He−Kr	3.20	40.94
Ar−Ar	3.41	120.00
Ne−Ar	3.08	65.36
He−Ar	2.99	35.02
Ne−Ne	2.75	35.60
He−Ne	2.66	19.07
He−He	2.56	10.22

Equations 2.5−2.9 comprise the VER integral formula for $\langle F^2\rangle_0$. Next, we give the diffusion integral formulas.

(ii) Formulas for the Diffusion Gaussian Parameters. The diffusion $\langle F^2\rangle_0$ formula can be directly compared with the corresponding VER formula of eq 2.5, so we give it first. It is

$$\langle F^2\rangle_0 = 4\pi\rho\int_0^{\infty} y^2\, g(y)\,[u'(y)]^2\,\mathrm{d}y \tag{2.10}$$

where y is the distance between the solute atom and a solvent atom and where $g(r)$ and $u(r)$ are the solute−solvent radial distribution functions and pair potentials.

The diffusion equation, 2.10, and the VER equation, 2.5, are very dissimilar. As one example, eq 2.10 is solute-mass-independent, whereas eq 2.5 depends on both solute atom masses. As a second example, eq 2.10 depends only on the solute−solvent separation y, whereas eq 2.5 depends not only on the separations y_1 and y_2 but also on the spherical polar angle, θ.

The diffusion $\langle \dot{F}^2\rangle_0$ formula, in contrast to the corresponding VER formula, is very simple and has the form,

$$\langle \dot{F}^2\rangle_0 = \frac{4\pi\rho}{M}k_B T\int_0^{\infty} y^2\, g(y)\,\{[u''(y)]^2 + [y^{-1}\,u'(y)]^2\}\,\mathrm{d}y \tag{2.11}$$

where M is the mass of a solvent atom. Next, we outline how we numerically evaluate the proceeding equations.

c. Numerical Procedures. Our computational methods for τ_{VER} are described in detail elsewhere.[8] The procedures used here for τ_{DIF} are nearly identical. In brief, after computing the $g(r)$'s from the Percus−Yevick integral equation, we evaluate eqs 2.10−2.11 by numerical quadrature. The computation times for both τ_{VER} and τ_{DIF} are negligible. Typically, computations of either τ over the whole solvent supercritical region (≈50 states) requires about 15 CPU seconds on a mainframe computer.

Next, in sections III and IV, we implement this computational method using the Lennard-Jones potentials of Table 1.[9] Specifically we numerically prove the isothermal ρ independence of the diffusion decay time, $\tau_{DIF.}$ In section III, we limit our proof to $T = 300$ K systems. Then in section IV, we lift this restriction and give results for temperatures as low as 15 K and as high as 1500 K.

TABLE 2: Decay Times τ_{VER} (fs)[a] for H_2 and D_2 at Infinite Dilution in a ^{40}Ar Solvent at $T = 300$ K[b]

	PF						
$T = 300$ K	0.0001	0.01	0.05	0.1	0.2	0.3	0.4
	τ_{VER} (fs)						
H_2-Ar	5.48	5.48	5.48	5.48	5.48	5.48	5.48
D_2-Ar	7.40	7.40	7.40	7.40	7.40	7.40	7.40

[a] τ_{VER} is *not* the VER time T_1. [b] For both solutions, τ_{VER} is ρ- or equivalently packing fraction (PF)-independent. PF is defined in terms of the density ρ as $PF = 1/6\pi\rho\sigma_{vv}^3$, where σ_{vv} is the solvent Lennard-Jones σ.

TABLE 3: Diffusion of Rare Gas Solutes at Infinite Dilution in Rare Gas Solvents at $T = 300$ K[a]

	PF						
solution	0.0001	0.01	0.05	0.1	0.2	0.3	0.4
	τ_{DIF} (fs) at 300 K						
Xe−Xe	133.65	133.66	133.66	133.68	133.73	133.83	134.11
Kr−Xe	130.98	130.98	131.00	131.02	131.09	131.21	131.48
Ar−Xe	125.43	125.43	125.45	125.48	125.57	125.69	125.93
Ne−Xe	118.31	118.31	118.34	118.37	118.45	118.55	118.71
He−Xe	116.80	116.80	116.82	116.84	116.87	116.93	117.00
Xe−Kr	104.64	104.64	104.65	104.67	104.74	104.86	105.10
Kr−Kr	102.06	102.06	102.08	102.10	102.17	102.30	102.52
Ar−Kr	97.45	97.46	97.47	97.50	97.57	97.68	97.87
Ne−Kr	91.18	91.18	91.20	91.22	91.27	91.35	91.46
He−Kr	89.80	89.81	89.81	89.82	89.85	89.88	89.92
Xe−Ar	69.20	69.20	69.22	69.24	69.30	69.41	69.58
Kr−Ar	67.28	67.29	67.30	67.32	67.39	67.48	67.64
Ar−Ar	63.96	63.96	63.98	64.00	64.05	64.13	64.26
Ne−Ar	59.21	59.22	59.23	59.24	59.27	59.32	59.38
He−Ar	57.97	57.97	57.97	57.98	57.99	58.00	58.02
Xe−Ne	46.38	46.39	46.40	46.42	46.47	46.54	46.62
Kr−Ne	44.74	44.75	44.76	44.77	44.82	44.87	44.94
Ar−Ne	42.09	42.09	42.10	42.11	42.14	42.18	42.23
Ne−Ne	37.89	37.89	37.89	37.90	37.91	37.91	37.93
He−Ne	36.43	36.43	36.43	36.43	36.42	36.41	36.40
Xe−He	20.39	20.39	20.40	20.40	20.41	20.43	20.44
Kr−He	19.63	19.63	19.63	19.63	19.64	19.65	19.66
Ar−He	18.35	18.35	18.35	18.35	18.36	18.36	18.37
Ne−He	16.23	16.23	16.23	16.22	16.22	16.22	16.21
He−He	15.34	15.34	15.34	15.34	15.33	15.32	15.31

[a] For a pair A−B, A is the solute, and B is the solvent. Notice all τ_{DIF}'s are nearly PF-independent. Results are for the common rare gas isotopes.

III. τ_{VER} and τ_{DIF} ρ Independence at 300 K

To emphasize the generality of isothermal τ constancy, we first give a typical example of our earlier extensive results for VER.[1] Then we give our new results for diffusion.

a. Constancy of τ_{VER} for H_2/Ar and D_2/Ar Solutions. Concerning VER, Table 2 shows for the representative H_2/Ar and D_2/Ar solutions at $T = 300$ K that density or packing fraction (PF) independence holds for τ_{VER} over the whole range of ideal gas ($PF = 10^{-4}$) to dense fluid ($PF = 0.4$).

b. Constancy of τ_{DIF} for Rare Gas Systems. Next, we summarize the results for τ_{DIF} for all 25 rare gas combinations. We have computed τ_{DIF}'s for 1715 thermodynamic states of these systems cover the full ρ of range ideal gas to dense fluid over a broad range of Ts. Our computations show that τ_{DIF} is isothermally ρ-independent for all systems and states to within 0.56%. The largest deviations occur for the highest ρ's, which correspond to $PF = 0.4$.

To provide a manageable sample of these 1715 τ_{DIF} values, in Table 3, we give the $T = 300$ K τ_{DIF}'s. These 300 K results illustrate the points just made.

However we can give our full T-dependent results for a few systems. We next describe these results. (The results not published here are posted elsewhere.[10])

IV. T- and ρ Dependencies of τ_{DIF} for Four Supercritical Rare Gas Fluids

Specifically, we study the T and ρ dependencies of τ_{DIF} for four supercritical rare gas systems. We start with the He−He and Xe−Xe fluids, which are especially interesting, since they are the most divergent of our rare gas systems.

a. The He−He and Xe−Xe Systems. The divergent nature of the He−He and Xe−Xe fluids is evident from Figure 1, which shows that the LJ potentials for the two systems are radically different. Especially conspicuous in Figure 1 are the large differences in the magnitude of the well depths and the location of the repulsive walls of these two potentials. Unsurprisingly, the two LJ potentials yield the very different $g(r)$'s. This is illustrated in Figure 2, which gives the plots of these $g(r)$'s at $T = 300$ K.

Despite the dissimilarities evident in Figures 1 and 2, Tables 4 and 5 reveal that both the He−He and Xe−Xe systems show isothermal ρ independence over the supercritical region of their phase diagrams.

Specifically, for the He−He system, Table 4 establishes that isothermal ρ independence of τ_{DIF} holds for the 2 orders of magnitude T range 15−1500K, since it shows that over this whole range, the maximum percent deviation from perfect constancy is 0.48%.

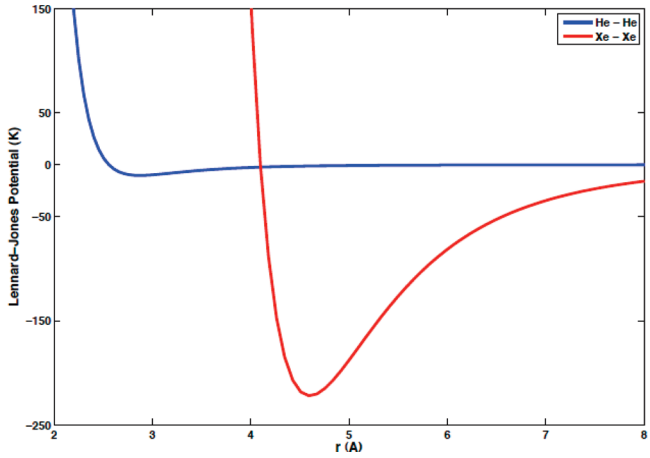

Figure 1. Lennard-Jones potentials for He−He and Xe−Xe. Even though these potentials are radically disparate, both yield τ_{DIF} constancy (Tables 4 and 5).

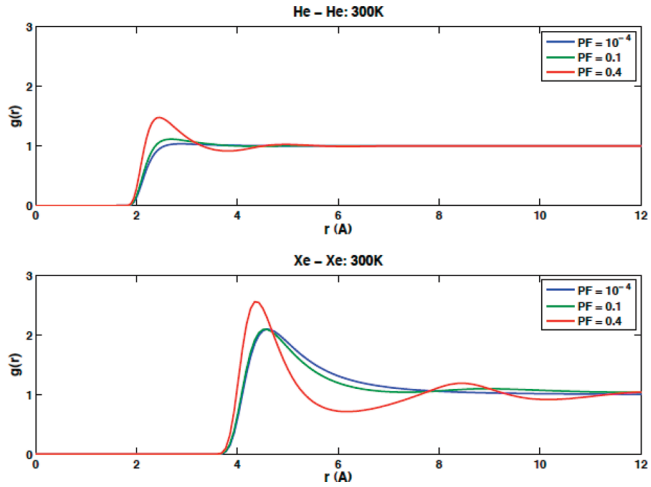

Figure 2. Pair correlation functions $g(r)$ at $T = 300$ K for the systems of Figure 1. (a) He−He at three PFs and (b) Xe−Xe at three PFs.

Turning to Table 5 for the Xe−Xe system, one sees that isothermal ρ independence of τ_{DIF} holds for the T range 300−1500 K. This is made especially clear by the percent error plots of Figure 3, which show that the percent deviations of τ_{DIF} from perfect constancy are very small. Specifically, for the temperatures 300, 800, and 1500 K, the maximum deviation from perfect constancy occurs at 800 K and is 0.39%. Including all of the Ts of Table 5, the maximum deviation for the Xe−Xe system is 0.46% and occurs for $T = 600$ K.

Next, we turn to a graphical study of the Kr−Kr and Ar−Ar systems.

b. The Kr−Kr and Ar−Ar Systems. First, Figure 4 establishes for the Kr−Kr system ρ independence at temperatures 300, 800, and 1500 K. Thus, Figure 4 extends the Kr−Kr results of 300 K given in Table 3 to higher Ts.

Next, in Figure 5, for Kr−Kr and Ar−Ar fluids, we plot the T dependence of τ_{DIF} over the range 300−1500 K. These plots show that for these fluids, τ_{DIF} is strongly T-dependent. In addition, the plots further confirm ρ independence, since each plot is a superposition of indistinguishable τ_{DIF} plots for each of the PFs of Figure 3.

In summary, the results of Tables 3−5 and Figures 3−5 establish that τ_{DIF} is isothermally ρ-independent for all systems consisting of a diffusing solute atom in an otherwise pure rare gas solvent.

V. Discussion

We deal with three topics in this section. The first is the development of the liquid−gas correlation relation for the diffusion coefficient $D(T, \rho)$. The second is to link the isothermal ρ independence of τ_{DIF} to inertial solvent dynamics.[5] The third is to make contact with the related work of others.[11]

a. The l−g Correlation Equation for $D(T, \rho)$. To demonstrate the parallel between VER and diffusion correlation relations, we first review our theoretical l−g correlation formula for the VER rate constant, $k(T, \rho)$. This formula was derived[1] from the τ_{VER} ρ independence as

$$k(T,\rho_l) = \left(\frac{\rho_l}{\rho_g}\right) k(T,\rho_g) \left[\frac{\rho_l^{-1}\langle F^2\rangle_{0,l}}{\rho_g^{-1}\langle F^2\rangle_{0,g}}\right] \tag{2.12}$$

Equation 2.12 not only provides a foundation for the phenomenological eq 1.1, it also yields the following theoretical formula for its empirical parameter, G.

$$G = \left[\frac{\rho_l^{-1}\langle F^2\rangle_{0,l}}{\rho_g^{-1}\langle F^2\rangle_{0,g}}\right] \tag{2.13}$$

A formula analogous to eq 2.12 holds for $D(T, \rho)$; namely,

$$D^{-1}(T,\rho_l) = \left(\frac{\rho_l}{\rho_g}\right) D^{-1}(T,\rho_g) \left[\frac{\rho_l^{-1}\langle F^2\rangle_{0,l}}{\rho_g^{-1}\langle F^2\rangle_{0,g}}\right] \tag{2.14}$$

We next derive eq 2.14. We start with the Einstein relation $D(T, \rho) = k_B T/\beta$, where $\beta = \beta(T, \rho)$ is the solute atom's friction coefficient, written in the form

$$D^{-1}(T,\rho) = \frac{\beta}{k_B T} \tag{2.15}$$

To evaluate eq 2.15, we derive a molecular formula for β. For simplicity, we restrict the derivation by using the approximate Gaussian faf $C_G(t)$ of eq 2.4. To start, we use the standard relationship between the friction kernel, $\beta(t)$, and the normalized faf, $C(t)$:

$$\beta(t) = \frac{\langle F^2\rangle_0}{k_B T} C(t) \tag{2.16}$$

The friction coefficient β is given in terms of $\beta(t)$ as

$$\beta = \int_0^\infty \beta(t)\, dt = \frac{\langle F^2\rangle_0}{k_B T} \int_0^\infty C(t)\, dt \tag{2.17}$$

Evaluating eq 2.17 using $C_G(t)$ gives β as $\beta = (\pi/2)^{1/2}\tau(\langle F^2\rangle_0/k_B T)$, which from eq 2.15 yields the following Gaussian approximation to $D^{-1}(T, \rho)$,

$$D^{-1}(T,\rho) = \left(\frac{\pi}{2}\right)^{1/2} \frac{\langle F^2\rangle_0}{(k_B T)^2}\tau \tag{2.18}$$

TABLE 4: PF and T Dependencies of τ_{DIF} for the He−He System[a]

	PF						
T (K)	0.0001	0.01	0.05	0.1	0.2	0.3	0.4
	τ_{DIF} (fs)						
15	65.60	65.60	65.61	65.62	65.65	65.71	65.86
50	38.22	38.23	38.23	38.24	38.26	38.30	38.34
100	27.21	27.21	27.21	27.21	27.21	27.22	27.22
200	19.03	19.03	19.03	19.03	19.02	19.01	19.01
300	15.34	15.34	15.34	15.34	15.33	15.32	15.31
400	13.14	13.14	13.13	13.13	13.12	13.12	13.11
600	10.53	10.53	10.53	10.52	10.52	10.51	10.50
800	8.98	8.98	8.98	8.98	8.97	8.96	8.96
1000	7.93	7.93	7.93	7.93	7.92	7.92	7.91
1200	7.17	7.17	7.16	7.16	7.16	7.15	7.15
1500	6.32	6.32	6.32	6.32	6.31	6.31	6.30

[a] The τ_{DIF}'s are nearly PF-independent.

TABLE 5: Same as Table 4 Except for Xe−Xe from $T = 300$ to 1500 K

	PF						
T (K)	0.0001	0.01	0.05	0.1	0.2	0.3	0.4
	τ_{DIF} (fs)						
300	133.65	133.66	133.66	133.68	133.73	133.83	134.11
400	118.30	118.31	118.33	118.36	118.44	118.58	118.84
600	98.99	98.99	99.02	99.05	99.13	99.26	99.45
800	86.83	86.83	86.85	86.88	86.94	87.04	87.17
1000	78.23	78.23	78.25	78.27	78.32	78.39	78.48
1200	71.72	71.72	71.74	71.75	71.79	71.84	71.90
1500	64.36	64.36	64.37	64.38	64.40	64.43	64.47

From eq 2.18, it follows that

$$\frac{D^{-1}(T,\rho_l)}{D^{-1}(T,\rho_g)} = \frac{\tau_l\langle F^2\rangle_{0,l}}{\tau_g\langle F^2\rangle_{0,g}} \tag{2.19}$$

However, because τ_{DIF} is isothermally ρ-independent (Tables 3−5 and Figures 3−5), at any T,

$$\tau_l = \tau_g \tag{2.20}$$

Equations 2.19 and 2.20 are equivalent to eq 2.14. Thus, within the Gaussian approximation of eq 2.4 we have derived the l−g correlation relation of eq 2.14. Later, we will examine the validity of this model.[7]

Next we link the ρ independence of the decay times, τ, to inertial dynamics.

b. τ Constancy and Inertial Dynamics. Consider a particle of mass m and coordinate $x(t)$ subject to a force $F(t)$. Classical mechanics predicts that at the shortest times, $F(t)$ does not affect the particle's motion. Equivalently, at the shortest times, the particle moves as if it were free, and therefore, it has the trajectory

$$x(t) = x(t=0) + \dot{x}(t=0)t \tag{2.21}$$

As an example of how eq 2.21 emerges, suppose the particle is moving in a gravitational field so that $F(t) = mg$. Then its exact trajectory is

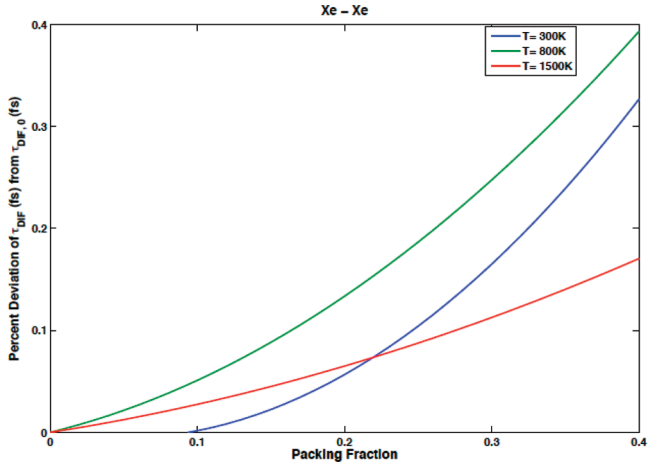

Figure 3. Percent deviation of τ_{DIF} at PF > 0 from $\tau_{DIF,0} = \tau_{DIF}$ (PF = 0) for Xe−Xe at T = 300, 800, and 1500 K. Percent deviation = $\tau^{-1}{}_{DIF,0}|\tau_{DIF}$ (PF) − $\tau_{DIF,0}| \times 100$. The maximum deviation is <0.4%, showing that τ_{DIF} (PF) is nearly PF-independent.

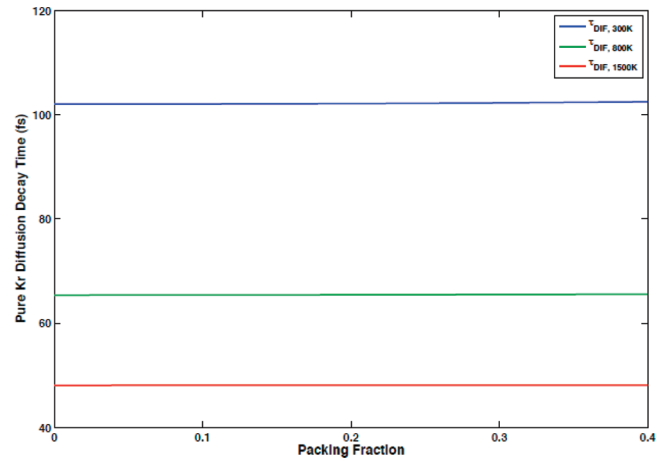

Figure 4. Diffusion decay times at temperatures 300, 800, and 1500 K vs PF for the representative Kr−Kr system. The decay time, τ_{DIF}, is (nearly) PF-independent over the whole range ideal gas to dense fluid.

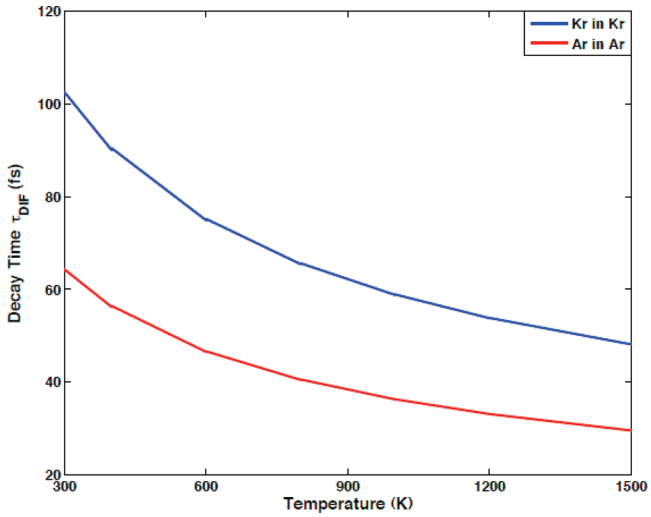

Figure 5. τ_{DIF} vs T (K) for the Kr−Kr and Ar−Ar systems. All curves are plotted over the PF range of Figure 3. However, graphs for different PFs are superposed, again showing PF independence of τ_{DIF}.

$$x(t) = x(t = 0) + \dot{x}(t = 0)t + \frac{1}{2}gt^2 \qquad (2.22)$$

However, at the shortest times, the $(1/2)gt^2$ term in eq 2.22 is negligible compared with the other two terms, and therefore, eq 2.22 reduces to the free particle equation, 2.21. The shortest time force free motion of eq 2.21 is called *inertial motion*.[5]

Next, let us apply these concepts to the motion of solvent atoms around a solute atom. These concepts imply that at the shortest times, a solvent atom feels no force from either the solute atom or other solvent atoms. Therefore, at these times, each solvent atom moves like a free particle, and as a result, the short time motions of each solvent atom are ρ-independent.

Since the solvent motion is what causes the decay of $\langle F(t)F\rangle_0$, the ρ independence of the solvent's inertial motion is the basis of the ρ independence of τ. However there is one additional factor. Although the solvent inertial motions are ρ-independent, they are T-dependent. This follows since the root-mean-square initial velocity of each solvent atom is T-dependent. As a consequence, whereas τ is ρ-independent at each T, it is T-dependent at each ρ.

In brief, $\tau = \tau(T, \rho) = \tau(T)$.

c. Related Work. There is a paucity of information about the isothermal ρ dependencies of faf's. Moreover, the existing information is solely for VER. The most detailed data appears in Figures 2 and 3 of a paper by Chesnoy and Weis.[11a] In their Figure 2, they plot normalized molecular dynamics (MD) faf's for VER in a Lennard-Jones (LJ) solvent. The faf's are for a single T, but cover a 3-fold ρ range. Like us, Chesnoy and Gale found ρ independence at the shortest times. In their Figure 3, they plot the frequency spectra of these faf's up to wavenumbers $\tilde{\omega} \cong 125$ cm^{-1}. The spectra seem to be ρ-independent for $\tilde{\omega} \gtrsim 60$ cm^{-1}. These results are hardly conclusive, but they accord with our proof[1] that the high ω asymptotes of faf frequency spectra depend solely on the ρ-independent decay time, τ.

Simpson and co-workers[11b] provide related MD simulation results and analysis in their sections 4 and 5. They conclude the following: "*At large values* $\tilde{\Delta\nu}$ [corresponding to our $\tilde{\omega}$] *the* **very short time** *characteristics of the correlation function* [faf] *are reflected in the value of the Fourier transform* [frequency spectrum] *and hence* k_L *and* k_G [$k[T, \rho_l]$ and $k[T, \rho_g]$ of eq 1.1]." They then show from their simulations that the dynamical part of their correlation functions (our $C[t]$) is ρ-independent at the shortest times. They then use these results to justify correlation relations such as eq 1.1. These findings are summarized in their Figure 3.

Further evidence for the isothermal ρ independence of τ comes from MD simulations and theoretical analysis of Egorov and Skinner.[11c] In their Figures 2 and 4, they plot two $C(t)$'s at the same reduced T but at two reduced densities. The plots appear identical at the shortest times.

Supporting Information Available: This material is available free of charge via the Internet at http://pubs.acs.org.

References and Notes

(1) Adelman, S. A. *J. Phys. Chem. A* **2010**, *114*, 5231.

(2) Equation 1.1 is usually rationalized using the IBC model. See Chesnoy, J.; Gale, G. M. *Ann. Phys. (Paris, Fr.)* **1984**, *9*, 893, and references within.

(3) The subscript 0 in $\langle F(t)F\rangle_0$ denotes that the solute is fixed in the liquid. This fixing constraint is a specialization of our partial clamping model constraints. This model is simply described in Adelman, S. A.; Stote, R. H.; Muralidhar, R. *J. Chem. Phys.* **1993**, *99*, 1320, where references to the papers which develop the model are given.

(4) For comprehensive treatments of diffusion, see, for example, Middleman, S. *An Introduction to Mass and Heat Transfer: Principle of Analysis and Design*: John Wiley & Sons, Inc.: New York, 1998; especially Chapter 2; Cussler, E. L. *Diffusion Mass Transfer in Fluid Systems*, 2nd ed.; Cambridge University Press: New York, 1997.

(5) Inertial motions may have first become prominent in physical chemistry in the context of time-dependent solvation phenomena. For a comprehensive review with many references, see: Fleming, G. R.; Cho, M. *Ann. Rev. Phys. Chem.* **1996**, *47*, 104.

(6) For VER, the integral formulas are derived and summarized in Adelman, S. A.; Ravi, R.; Muralidhar, R.; Stote, R. H. *Adv. Chem. Phys.* **1993**, *84*, 73.

(7) For the diffusion processes studied, the integral formulas are derived by S.A. Adelman, unpublished notes.

(8) Adelman, S. A.; Muralidhar, R.; Stote, R. H. *J. Chem. Phys.* **1991**, *95*, 2738.

(9) The Lennard-Jones parameters for the interactions of identical rare gas pairs, such as Ar−Ar, are tabulated in many sources. The values listed in Table 1 are representative of most of these tabulations. We attempted to obtain the parameters for mixed pairs, such as Ar−Kr, using sophisticated combination rules such as those of Waldman, J.; Hagler, A. T. *J. Comput. Chem.* **1993**, *14*, 1097. However, these gave unphysical results. So we instead used the Berthelot−Lorentz (BL) rules $\sigma_{ij} = 0.5[\sigma_i + \sigma_j]$ and $\varepsilon_{ij} = (\varepsilon_i\varepsilon_j)^{1/2}$. The BL rules are known to be highly inaccurate, but they are sufficient for our purposes here.

(10) Posted as supplementary material at http://pubs.acs.org.

(11) For other evidence for ρ independence of $\langle F(t)F\rangle_0$, see (a) Chesnoy, J.; Weis, J. J. *J. Chem. Phys.* **1986**, *84*, 5378. (b) Andrew, J. J.; Harriss, A. P.; McDermott, D. C.; Williams, H. T.; Madden, P. A.; Simpson, C. J. S. M. *Chem. Phys.* **1989**, *139*, 369. (c) Egorov, S. A.; Skinner, J. L. *J. Chem. Phys.* **1996**, *105*, 7047.

JP1074175